Quantitative Work Function Measurements on a Nanometer Scale: Kelvin Probe Force Microscopy in Ultrahigh Vacuum

Sascha Sadewasser

Hahn-Meitner Institut, Glienicker Str. 100, 14109 Berlin, Germany

Keywords: Atomic Force Microscopy, Work Function, Kelvin Probe Force Microscopy, Semiconductors

Abstract. The application of scanning probe microscopy has tremendously increased the understanding of materials, processes and physics on the nanometer scale. Besides the basic atomic force microscope, which measures a sample's surface topography, many specialized variations have been developed to obtain specific additional information. In this chapter we will discuss the Kelvin probe force microscope, which is designed to obtain laterally resolved images of a sample's work function by measuring the electrostatic forces. Operating the microscope in ultrahigh vacuum, even absolute work function measurements can be realized. The method of Kelvin probe force microscopy will be introduced and different measuring modes discussed. The amplitude modulation technique has the advantage of requiring only small sampling voltages, however, due to long range electrostatic forces the lateral resolution is limited. The frequency modulation technique on the other hand is sensitive to the force gradient, which provides better lateral resolution, but requires a much larger sampling voltage. After discussing advantages of operation in ultrahigh vacuum, several examples of recent applications of this technique will be reviewed.

Introduction

The discovery of the scanning tunneling microscope allowed for the first time to image sample surfaces with true atomic resolution [1, 2]. However, due to the working principle, namely the tunneling currents between tip and sample, its application is inherently restricted to conductive surfaces. With the invention of the atomic force microscope (AFM) a similar technique became available, which additionally allowed the measurement on non conductive samples [2, 3]. This opened a wide field of applications, from insulators, to biological samples and chemistry [2, 4, 5]. In addition to "just" measuring the sample's surface topography, it became also possible to measure additional surface properties by employing specialized tips, or using specific techniques. These scanning probe microscopes (SPM) enhance the possible applications even further, i.e. magnetic force microscopy allows to image magnetic properties by using a magnetically sensitive tip [6], conductive tips can be used to measure charge carrier distributions by the scanning capacitance technique [7], and friction on the atomic scale is studied by monitoring the lateral torsion of the cantilever [8].

In this chapter we want to focus on Kelvin probe force microscopy (KPFM), a technique that images the sample's work function [9, 10]. As the work function represents an important parameter in many fields, the KPFM represents an important tool for material and device characterization. By means of the work function, it also becomes possible to distinguish different materials on a sample. Already in 1898 Lord Kelvin developed the vibrating capacitor technique to investigate the surface electricity of metals [11]. The changing distance between two capacitor plates induces a current, which is minimized by applying a voltage that corresponds to the contact potential difference (CPD). The KPFM was first introduced by Weaver and Abraham [9] in 1991, and combined the macroscopic Kelvin probe with a non-contact AFM (NC-AFM). Since the AFM tip provides only a small area, the resulting currents would be too small for a reasonable detection. Since the AFM cantilever is designed as a very sensitive force probe, the KPFM uses electrostatic forces instead of currents. The KPFM operated in air found many applications, for example charge carrier profiling [12], and semiconductor device analysis [13]. However, to obtain absolute

work function values, operation in ultrahigh vacuum (UHV) is essential. Adsorbates contaminate the surface in air resulting in a modified work function [14, 15]. The UHV-KPFM was developed by Kikukawa *et al.* in 1995 [16, 17]. Besides transferring the setup into UHV, also the measurement technique had to be adjusted. Whereas for NC-AFM in air the amplitude of the oscillating cantilever is used to control the tip-sample distance, the higher quality factor in UHV requires using the oscillation frequency directly for the distance control [18]. So far, a much smaller number of studies has been conducted in UHV as compared to air-KPFM studies.

In this chapter we will present a setup of a KPFM in UHV, which achieves a lateral resolution of ~ 20 nm and energy resolution of ~ 5 meV [19]. We will show several applications of this experiment to semiconductor surfaces and devices. In the following section we will introduce the method of KPFM in detail, followed by a review of several studies that were conducted using UHV-KPFM.

Experiment

As most SPMs are based on the AFM, it is essential to first introduce its principle. A thorough description of SPM can be found in ref. [2]. The atomic force microscope uses a sharp tip at the end of a cantilever to image the surface of a sample. Two principle working modes can be distinguished, contact mode and non-contact mode. In contact mode, the tip is brought into contact with the sample and then scanned across its surface, while a laser beam, which is reflected off the back-side of the cantilever and read-out by a position sensitive photo diode, is used to measure changes in the cantilever position. Changes in the photo diode signal will be compensated by an appropriate vertical change in the position of the sample. Thus, the topography of the sample surface is imaged as the tip is scanned across the surface.

For NC-AFM the measurement relies on the change of the resonance frequency when forces act on the cantilever. By means of a piezo, the cantilever is oscillated at its resonance frequency. The oscillation is detected by the oscillating position of the reflected laser beam on the position sensitive photo diode. Is the tip approached to the sample close enough so that forces between the tip and the sample act, the resonance frequency is shifted. In order to maintain the tip-sample distance constant, two distinguished modes can be used. In the amplitude modulation technique (AM-mode) the tip-sample distance is changed so that the amplitude of the oscillation is maintained constant. For the frequency modulation technique (FM-mode) the frequency shift with respect to the free resonance frequency is maintained constant by adjusting the tip-sample distance. The fact that the cantilever is sensitive to the force gradient is responsible for the high resolution of SPM [2]. Due to the higher quality factor of the oscillation and the related rapid decease of the oscillation amplitude, the FM-mode has to be used in UHV [18].

The KPFM is based on a NC-AFM and the measurement of the work function employs the electrostatic forces between tip and sample. The cantilever is oscillated at its resonance frequency with a constant amplitude. A voltage is applied between tip and sample, consisting of a dc-bias U_{dc} and an ac-voltage $U_{ac}\ sin(\mathbf{w}\,t)$ at the frequency $\mathbf{w}$. The application of this voltage $U(t)$ results in an oscillating electrostatic force, inducing an additional oscillation of the cantilever at $\mathbf{w}$. Assuming the tip-sample system to be a capacitor, the electrostatic force is:

$$F_{es} = -\frac{1}{2}\frac{\partial C}{\partial z}U(t)^2 = -\frac{1}{2}\frac{\partial C}{\partial z}\left[U_{dc} - \frac{\Delta\Phi}{e} + U_{ac}\sin\left(\mathbf{w}t\right)\right]^2 , \qquad (1)$$

where e is the elementary charge, $\partial C/\partial z$ the gradient of the capacitance of the tip-sample system and $\Delta\Phi/e$ the CPD, which is the difference in work function between the tip and the sample. Eq. (1) can be written as $F_{es} = F_{dc} + F_{\mathbf{w}} + F_{2\mathbf{w}}$, with the spectral components:

$$F_{dc} = -\frac{\partial C}{\partial z}\left[\frac{1}{2}\left(U_{dc} - \frac{\Delta\Phi}{e}\right)^2 + \frac{U_{ac}^2}{4}\right] , \tag{2}$$

$$F_{\omega} = -\frac{\partial C}{\partial z}\left(U_{dc} - \frac{\Delta\Phi}{e}\right)U_{ac}\sin(\omega t) , \tag{3}$$

$$F_{2\omega} = \frac{\partial C}{\partial z}\frac{U_{ac}}{4}\cos(2\omega t) . \tag{4}$$

The dc part F_{dc} in Eq. (2) contributes to the topographical signal, the term F_{ω} at the ac-frequency ω in Eq. (3) is used to measure the CPD and the contribution $F_{2\omega}$ in Eq. (4) can be used for capacitance microscopy. Fig. 1 shows a schematic diagram of the electronics used for the UHV-KPFM. A lock-in amplifier is used to detect the cantilever oscillation at ω. This signal is minimized by applying the dc-bias U_{dc}, which corresponds to the CPD as can be seen from Eq. (3); recording U_{dc} with the scan gives an image of the CPD. Calibrating the tip against a sample (in our case we use highly oriented pyrolytic graphite – HOPG) with a known work function allows to derive the sample's work function. Also for the CPD measurement two distinct modes can be used, similar to the AM and FM-mode in the topography measurement. For the FM mode [16] the modulation of the frequency shift, induced by the applied ac-voltage, is measured with the lock-in amplifier, whereas in the AM-mode [10] the oscillation amplitude of the cantilever at ω is monitored with the lock-in amplifier. For the electrostatic force detection, the AM-mode detects the force directly, whereas the FM-mode is sensitive to the force gradient. Thus the FM-mode is expected to allow a better lateral resolution. However, higher ac-voltages are necessary in this mode. In our experimental setup, the ac-frequency ω is tuned to the second resonance frequency of the cantilever which results in an improved sensitivity and allows the independent and simultaneous imaging of the topography and CPD. An energy resolution of ~ 5 meV is obtained with ac-voltages as low as 100 mV. This allows application to semiconductors, where large ac-voltages could induce band bending at the surface, thereby falsifying the work function measurement.

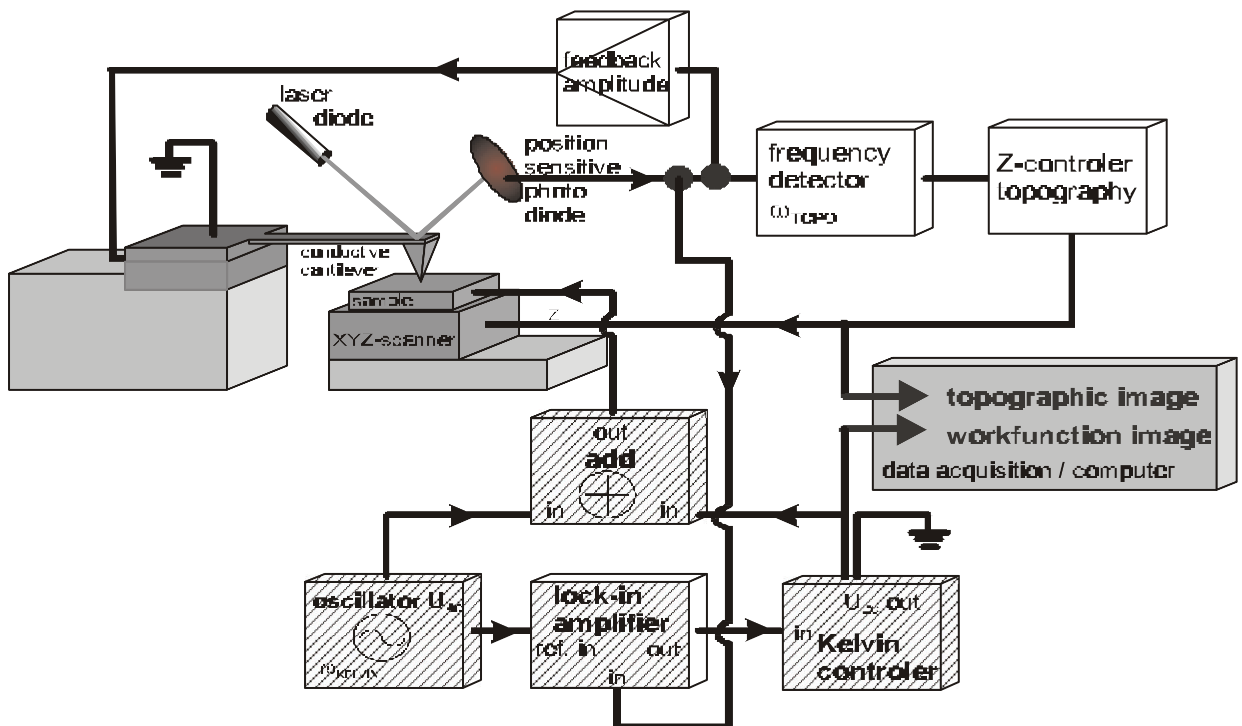

Fig. 1: *Schematic representation of the KPFM. The electronics represented with the shaded filling were added for the Kelvin mode of the microscope [20].*

Additional information about surface band bending can be obtained by the surface photovoltage (SPV) method. The sample is illuminated by either white light or a laser with a specific wavelength, resulting in charge carrier excitation. As the occupation of surface states changes, the surface band bending is changed, in most cases it is reduced. If the illumination intensity is sufficient, flat band conditions at the surface result [21].

Properties of the presented UHV-KPFM

The presented KPFM consists of a modified commercial Omicron UHV-AFM/STM, operated at a base pressure $p < 10^{-10}$ mbar. As described above, NC-AFM in UHV requires the use of the FM-mode [19,20,22] at the first cantilever resonance frequency for the topography measurement. Studies were conducted using the AM-mode for the CPD measurement, generally applying an ac-voltage as low as 100 mV to the sample. Unless stated otherwise, measurement of semiconductors are performed in darkness, to avoid unintentional excitation of the sample. We use commercially available cantilevers, which for most measurements (especially under illumination) are metal coated (PtIr or W_2C).

The proper operation of the KPFM was tested by measuring the CPD of a Si tip against various UHV prepared samples: n- and p-type GaAs were cleaved to expose the (110) surface, and HOPG was also cleaved in UHV [19]. Since the (110) surface of GaAs is free of surface states [23], it is in flat band condition. When plotting the CPD of these surfaces against the literature value of the work function (Fig. 2), the points can be fitted by a straight line with slope 1, indicating the one-to-one correspondence of the measured CPD with the work function of the material [19]. Also apparent from Fig. 2 is the importance of UHV preparation of the measured surfaces. The open circle corresponds to an air-cleaved HOPG sample, for which the CPD is ~ 0.5 eV lower as for the UHV-cleaved surface. This clearly shows the alteration of the work function due to surface adsorbates, and proves the necessity of UHV operation for the determination of reliable absolute work function measurements.

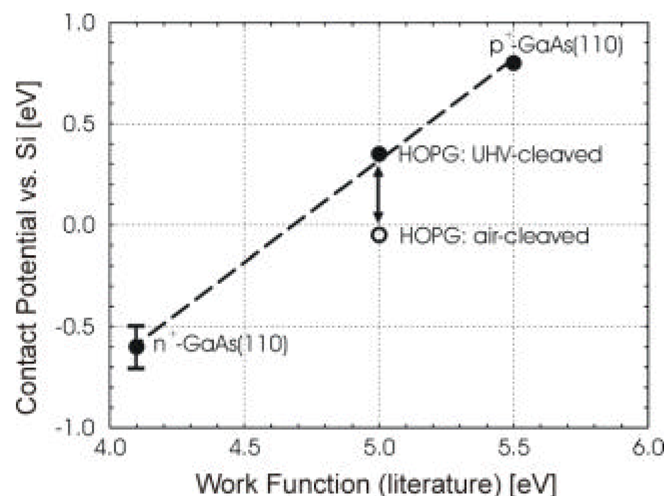

Fig. 2: *Plot of the measured CPD of several samples versus the literature value of the work function, showing the ability to measure absolute work function values once the cantilever (Si) is calibrated. Sample preparation in air results in adsorbates on the surface which seriously alter the work function as can be seen by the open circle. (reprinted from Ref. [19]).*

Review of UHV-KPFM studies

In this section a brief review of several UHV-KPFM studies is presented. Due to its well established preparation in UHV, a variety of studies has been performed on the Si(111) surface and on deposits on this surface. Several studies on solar cell materials have been conducted by our group.

Besides introducing the method for KPFM in vacuum, Kikukawa *et al.* also presented measurements on a Si pn structure [16,17]. Their microscope uses the AM-mode on the cantilever's 2nd resonance frequency for the CPD detection, and they report a lateral resolution for the CPD signal of 20 to 40 nm. The CPD difference between the p and n-type regions does not exceed 260 mV, and is therefore considerably lower than the expected difference, which should be close to the band gap of Si (high doping levels were used for the study). The origin for this discrepancy can be two-fold. The expected CPD contrast could be reduced due to surface contamination [24], either by the preparation of the surface by HF etching, or by the relatively high pressure (~ 10^{-5} mbar) of the vacuum. Secondly, an averaging effect of the cantilever has to be taken into account since the electrostatic forces are of long range nature. Thus, despite the reported resolution of 20 to 40 nm for the lateral contrast between p and n-type regions, the CPD contrast could be reduced.

Using the FM-mode for the detection of the electrostatic forces, Kitamura *et al.* [10,25,26] studied the surface of Si(111) with and without Ag or Au deposits. Their microscope operates in UHV ($p \approx 10^{-10}$ mbar), thus reducing the possible effect of surface adsorbates. Due to the FM detection, the tip is sensitive to the force gradient, which results in an improved lateral resolution. For Au/Si(111) they obtained atomically resolved topography images. In addition, from simultaneously obtained CPD images the authors assigned a 0.5 eV higher work function to the 5×2 phase as compared to the 7×7 phase [25]. Studying Ag deposited on Si(111), Kitamura *et al.* [26] observed a preferred formation of Ag-clusters on the faulted half of the 7×7 unit cells. They claimed atomic resolution for the CPD images and find the work function of the Ag clusters to be ~ 10 meV lower than that of the 7×7 structure.

Also using the FM detection for the electrostatic forces, Kobayashi *et al.* [27] studied C_{60} layers deposited by UHV evaporation on the Si(111) 7×7 reconstructed surface. With the enhanced resolution, they were able to observe CPD variations on the molecular scale. They distinguish different crystalline structures of the C_{60} film which show different CPD values. A lower CPD at the edges of the C_{60} film is attributed to a CPD variation due to a different charge distribution at the edge; however, also the possibility of an artifact originating from a crosstalk with the topography is considered.

Electron emission from scratched metal surfaces (a phenomenon called chemiemission), especially in atmospheres of reactive gases (i.e. O_2) is an important issue in the study of surface chemical reactivity. To explore the microscopic origin of this phenomenon, Nakayama *et al.* [28] studied the surface of Si(111) and scratched Si(111). They used the tip of the AFM to locally scratch the sample surface in a controlled fashion, and imaged the result using UHV-KPFM. Immediately after scratching the work function of the scratched region is higher as compared to the non-scratched regions. Subsequently, the sample was exposed to O_2 or N_2 gas with a pressure of $P = 10^{-8}$ mbar and the work function of both, scratched and non-scratched regions was observed as a function of exposure time. For the N_2 no significant change of the work function could be observed. However, for O_2 exposure, the work function of both regions was found to increase rapidly initially, and after going through a maximum a slight decrease was observed. The rate of the initial increase for the scratched region is lower, thus resulting in a contrast reversal of the work function images after extended oxygen exposure: the work function of the scratched region is higher than the non-scratched region after 90 min of oxygen exposure.

Ludeke *et al.* [29] used a UHV-KPFM for the observation of charges. They attributed the existence of brighter and darker regions in CPD images of SiO_2 on Si(111) to the location of charges trapped in defects in the material. Furthermore, from observing the same contrast change for many of the locations, they concluded that the charge is located at the interface between Si and SiO_2. The authors distinguish between positive and negative charges and additionally observe the charging of the defect states by changing the applied bias to the sample. The density of defects concluded from the KPFM images is in excellent

agreement with the density estimated from capacitance-voltage measurements, thus supporting their interpretation of the observations.

Zhang *et al.* [30] combined a UHV-KPFM study with a conductive AFM study to facilitate the interpretation of the obtained images. They investigated the surface of diamond like carbon (DLC) films. Applying a voltage between tip and sample and measuring the current, they observed conductive and non conductive regions. The conductive regions are assumed to be of graphite structure whereas the diamond structure of the DLC film shows an insulating characteristic. Performing a KPFM scan on the same area as the conductive AFM, they obtained also the CPD for the surface. By superposition of the current image with the CPD image a correlation is made between conductive regions (with current flow) and regions with a low work function. However, from the same images it can be seen that other regions with a similarly low work function do not show conductive behavior. Thus, a direct correlation between conductive properties and work function seems critical.

An application of UHV-KPFM to an electronic device was presented very recently by Bürgi *et al.* [31], who studied a polymer thin film field-effect transistor. The active layer of their device consists of a spin-coated poly(3-hexylthiophene) and the authors measured the potential drop from the source across the active region to the drain depending on the applied voltages on source and drain. From these characteristics they extract field-effect mobilities for the device and find the results to agree with those from transistor characteristics, however, in their case obtained from a non-contact potentiometry measurement avoiding any undesired effects from contact resistances.

Sommerhalter *et al.* [19] reported the observation of a dipole located at the step edge of a HOPG surface. This dipole is due to the distribution of electronic charge at the step edge and results in a lower work function. This effect is well known from macroscopic measurements on stepped surfaces, showing lower work functions than atomically flat ones. The authors also report a variation of the work function at step edges when measuring on UHV cleaved (110) surfaces of p and n-type GaAs. In this case a work function increase is observed for n-type material (Fig. 3) and a decrease for the p-type GaAs. The (110) surface of GaAs is free of surface states [23] and therefore in flat band condition. However, the surface symmetry is interrupted at steps, which results in surface states. The topography in Fig. 3 (a) shows two monolayer steps across the surface of n-type GaAs, which was prepared by cleavage in UHV. The work function image in Fig. 3 (b) shows a higher work function along these steps. This effect can be understood considering the existence of charged surface states located at the step, which cause an upward band bending [19].

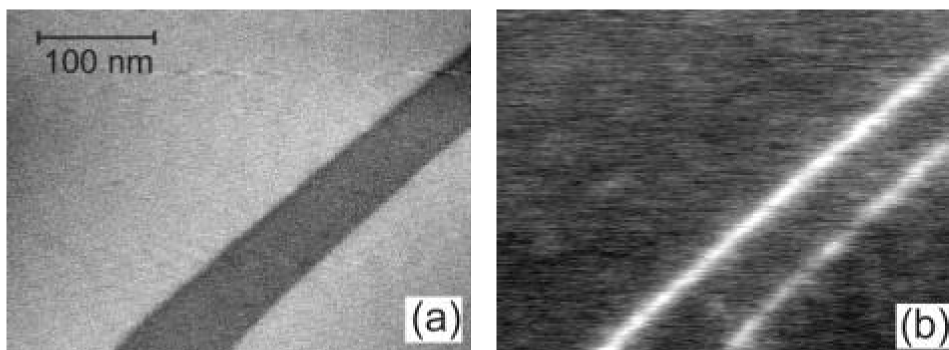

Fig. 3: *UHV cleaved (110) surface of n-type GaAs. The topography (a) shows two monolayer steps (Δz = 0.45 nm) along which the work function (b) increases by ~ 45 meV, explained by a surface state induced band bending. (reprinted from ref. [19])*

In the same paper, Sommerhalter *et al.* [19] studied the surface of UHV-cleaved p-type WSe_2 (0001). In the CPD image they observed several dark and bright spots, whereas the topography shows an atomically flat surface. The contrast in the CPD image was attributed to charged acceptor and donor sites, and their density corresponds well with results for carrier density and compensation from Hall

measurements. This example shows the ability of the KPFM to image the screened Coulomb potential of single charges.

A variety of studies on chalcopyrite solar cell materials has been performed by our group [32-37]. A few of these studies will be briefly described.

In a recent study, Sadewasser *et al.* [32] studied the band alignment between a ZnSe single crystal and a $CuGaSe_2$ absorber layer, as a model system for the absorber/buffer interface in chalcopyrite solar cells. By studying the electronic properties of the substrate and the absorber surface, i.e. the work function and the SPV, the band offset between absorber and buffer material was estimated using a formalism initially proposed by Kronik *et al.* [38] for macroscopic SPV measurements. In the same study the authors found lateral inhomogeneities in the $CuGaSe_2$ film, which became evident through a negative SPV of one grain, whereas the rest of the surface showed a positive SPV.

Another study was performed on the surface of $CuGaSe_2$ absorber material, also grown on a ZnSe (110) substrate [33]. The film was of polycrystalline nature, however, x-ray diffraction showed its orientation along the (220) direction. In the KPFM study, the work function on differently oriented facets of the grains was found to exhibit distinct values with differences between the facets as small as 30 meV up to 255 meV (Fig. 4). The differences were explained by a different surface dipole, determined by the orientation and termination of the surface. Moreover, due to the oriented growth, it was possible to determine the orientation of the facets, thereby allowing the assignment of the work function values to the surface orientation.

In a very recent study, Glatzel *et al.* [34] investigated the cross section through a complete solar cell device consisting of a $CuGaSe_2$ absorber, a CdS buffer layer and a ZnO window. The sample for the KPFM investigation was prepared by polishing, successfully avoiding the problem of large topographical height differences. To obtain clean surface conditions for the measurement of representative work function values, the sample was cleaned in UHV by argon sputtering. Besides clearly showing the various layers and their work function, also an additional $MoSe_x$ layer was found, whose formation was attributed to the reactive Se atmosphere during the chemical vapor deposition of the absorber.

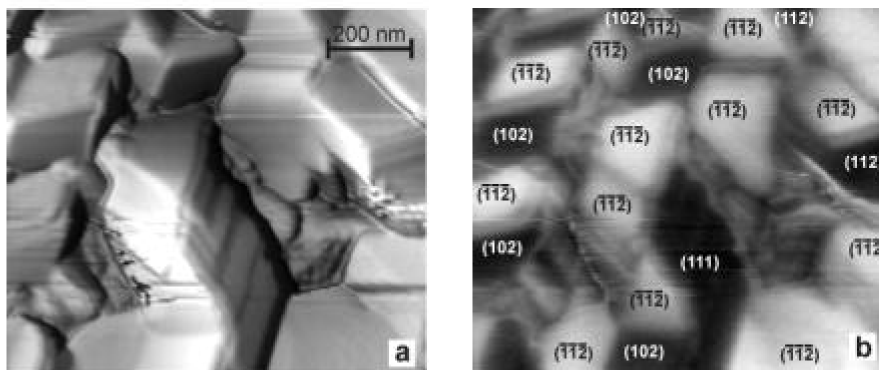

Fig. 4: *KPFM measurement of a $CuGaSe_2$ thin film on a ZnSe(110) substrate. (a) The topography showing distinct crystal facets on the (220) oriented film (Δz=384 nm). (b) The simultaneously measured work function shows constant values for the various facets (Φ=4.85...5.09 eV). The crystallographic orientation of the facets is assigned based on the angles to other facets and to the surface normal. (reprinted from ref. [34])*

Summary

Kelvin probe force microscopy in ultrahigh vacuum was presented as a special application of scanning probe microscopy that allows work function measurements with high lateral and energy resolution. The method was introduced explaining the different working modes that can be applied for experiments.

Several studies applying this technique were described, including a variety of experiments on Si(111), and several studies of chalcopyrite solar cell materials. It became clear that the Kelvin probe force microscope operated in ultrahigh vacuum represents an ideal tool for the characterization of semiconducting materials and devices. Since this technique is still quite young, the number of studies is limited, however, the increasing interest in this technique promises further application for the future.

The author acknowledges help and support from Th. Glatzel, Th. Matthes, Ch. Sommerhalter and M. Ch. Lux-Steiner.

References

[1] G. Binnig and H. Rohrer, Helv. Phys. Acta **55**, 726 (1982).
[2] R. Wiesendanger, *Scanning Probe Microscopy and Spectroscopy: Methods and Applications* (Cambridge Univ. Press, Cambridge, 1994).
[3] G. Binnig, C. F. Quate, and Ch. Gerber, Phys. Rev. Lett. **56**, 930 (1986).
[4] G. Binnig and H. Rohrer, Rev. Mod. Phys. **71**, S324 (1999).
[5] H. G. Hansma *et al.*, J. Struct. Biol. **119**, 99 (1997).
[6] Y. Martin and H. K. Wickramasinghe, Appl. Phys. Lett. **50**, 1455 (1987).
[7] J. R. Matey and J. Blanc, J. Appl. Phys. **57**, 1437 (1985).
[8] C. M. Mate, G. M. McClelland, R. Erlandsson, and S. Chiang, Phys. Rev. Lett. **59**, 1942 (1987).
[9] J. M. R. Weaver and D. W. Abraham, J. Vac. Sci. Technol. B **9**, 1559 (1991).
[10] S. Kitamura and H. Iwatsuki, Appl. Phys. Lett. **72**, 3154 (1998).
[11] L. Kelvin, Phil. Mag. **46**, 82 (1898).
[12] G. Koley and M. G. Spencer, J. Appl. Phys. **90**, 337 (2001).
[13] M. Tanimoto and O. Vatel, J. Vac. Sci. Technol. B **14**, 1547 (1996).
[14] M. S. Jean, S. Hudlet, and C. Guthmann, J. Berger, Phys. Rev. B **56**, 15391 (1997).
[15] M. Nonnenmacher, M. P. O'Boyle, and H. K. Wickramasinghe, Appl. Phys. Lett. **58**, 2921 (1991).
[16] A. Kikukawa, S. Hosaka, and R. Imura, Appl. Phys. Lett. **66**, 3510 (1995).
[17] A. Kikukawa, S. Hosaka, and R. Imura, Rev. Sci. Instrum. **67**, 1463 (1996).
[18] T. R. Albrecht, P. Grütter, D. Horne, and D. Rugar, J. Appl. Phys. **69**, 668 (1991).
[19] Ch. Sommerhalter, Th. W. Matthes, Th. Glatzel, A. Jäger-Waldau, and M. Ch. Lux-Steiner, Appl. Phys. Lett. **75**, 286 (1999).
[20] Ch. Sommerhalter, Dissertation, Freie Universität Berlin (1999).
[21] L. Kronik and Y. Shapira, Surf. Sci. Rep. **37**, 1 (1999).
[22] Ch. Sommerhalter, Th. Glatzel, Th. W. Matthes, A. Jäger-Waldau, and M. Ch. Lux-Steiner, Appl. Surf. Sci. **157**, 263 (2000).
[23] A. Huisjer and J. van Laar, Surf. Sci. **52**, 202 (1975).
[24] R. Shikler, T. Meoded. N. Fried, B. Mishori, and Y. Rosenwaks, J. Appl. Phys. **86**, 107 (1999).
[25] S. Kitamura, K. Suzuki, and M. Iwatsuki, Jpn. J. Appl. Phys. **37**, 3765 (1998).
[26] S. Kitamura, K. Suzuki, and H. Iwatsuki, Appl. Surf. Sci. **140**, 265 (1999).
[27] K. Kobayashi, H. Yamada, T. Horiuchi, and K. Matsushige, Jpn. J. Appl. Phys. **39**, 3827 (2000).
[28] K. Nakayama and L. Zhang, Jpn. J. Appl. Phys. **39**, 4509 (2000).
[29] R. Ludeke and E. Cartier, Appl. Phys. Lett. **78**, 3998 (2001).
[30] L. Zhang, T. Sakai, N. Sakuma, T. Ono, and K. Nakayama, Appl. Phys. Lett. **75**, 3527 (1999).
[31] L. Bürgi, H. Sirringhaus, and R. H. Friend, Appl. Phys. Lett. **80**, 2913 (2002).
[32] S. Sadewasser, Th. Glatzel, M. Rusu, A. Jäger-Waldau, and M.Ch. Lux-Steiner, Mater. Res. Soc. Symp. Proc. **668**, H5.4.1 (2001).

[33] S. Sadewasser, Th. Glatzel, M. Rusu, A. Jäger-Waldau, and M.Ch. Lux-Steiner, Appl. Phys. Lett. **80**, 2979 (2002).

[34] Th. Glatzel, D. Fuertes Marrón, Th. Schedel-Niedrig, S. Sadewasser, and M. Ch. Lux-Steiner, submitted to Appl. Phys. Lett. (2002).

[35] Ch. Sommerhalter, S. Sadewasser, Th. Glatzel, Th. W. Matthes, A. Jäger-Waldau, and M. Ch. Lux-Steiner, Surf. Sci. **482-485**, 1362 (2001).

[36] S. Sadewasser, Th. Glatzel, M. Rusu, A. Jäger-Waldau, and M. Ch. Lux-Steiner, Proc. of the 17th European Photovoltaic Solar Energy Conference, (München, 2001), p. 1155.

[37] Th. Glatzel, S. von Roon, S. Sadewasser, R. Klenk, A. Jäger-Waldau, and M. Ch. Lux-Steiner, Proc. of the 17th European Photovoltaic Solar Energy Conference (München, 2001), p. 1151.

[38] L. Kronik, L. Burstein, M. Leibovitch, Y. Shapira, D. Gal, E. Moons, J. Beier, G. Hodes, D. Cahen, D. Hariskos, R. Klenk, and H.-W. Schock, Appl. Phys. Lett. **67**, 1405 (1995).